

# Stimulated Raman backscattering of laser radiation in deep plasma channels

S. Yu. Kalmykov<sup>a)</sup> and G. Shvets

*Department of Physics and Institute for Fusion Studies, The University of Texas at Austin, Austin, Texas 78712*

(Received 26 December 2003; accepted 9 June 2004; published online 16 September 2004)

Stimulated Raman backscattering (RBS) of intense laser radiation confined by a single-mode plasma channel with a radial variation of plasma frequency greater than a homogeneous-plasma RBS bandwidth is characterized by a strong transverse localization of resonantly driven electron plasma waves (EPW). The EPW localization reduces the peak growth rate of RBS and increases the amplification bandwidth. The continuum of nonbound modes of backscattered radiation shrinks the transverse field profile in a channel and increases the RBS growth rate. Solution of the initial-value problem shows that an electromagnetic pulse amplified by the RBS in the single-mode deep plasma channel has a group velocity higher than in the case of homogeneous-plasma Raman amplification. Implications to the design of a RBS pulse compressor in a plasma channel are discussed. © 2004 American Institute of Physics. [DOI: 10.1063/1.1778743]

## I. INTRODUCTION

Stimulated Raman backscattering (RBS) of laser radiation in plasmas<sup>1</sup> is a parametric process in which a laser beam (pump wave) is backscattered off the electron plasma density fluctuations. These density perturbations are driven and amplified by the ponderomotive beat wave of pump and scattered electromagnetic (EM) waves. Under certain phase matching conditions, a positive feedback loop develops that results in the onset of a temporal or spatiotemporal instability.<sup>2</sup> The RBS in transversely homogeneous plasmas has been extensively studied since the early 1970s,<sup>1,2</sup> when it first came to the fore in the context of fast electron generation and target preheat in laser confinement fusion. The basic treatment of the RBS in homogeneous plasmas is now a classic that can be found in a number of textbooks.<sup>3</sup>

Although RBS of long laser beams has been studied for at least three decades, the short-pulse regimes of this instability have only recently attracted attention due to the advances in generation and amplification of ultrashort laser pulses.<sup>4</sup> The RBS of such pulses in rarefied homogeneous plasmas ( $\omega_p \ll \omega_0$ , where  $\omega_0$  is a fundamental frequency of laser,  $\omega_p = \sqrt{4\pi e^2 n_0 / m_e}$  is an electron Langmuir plasma frequency,  $-|e|$  is an electron charge, and  $n_0$  is an electron plasma density) has been explored in detail in both experiment<sup>5-10</sup> and theory.<sup>11-17</sup> The recent upsurge of interest in the RBS has been specifically caused by the theoretical discovery of the possibility to amplify and compress ultrashort laser pulses in plasma by backscattering a long low-intensity counterpropagating laser beam.<sup>18-20</sup>

Some applications of short-pulse lasers, such as novel x-ray source development,<sup>21</sup> generation of high harmonics of laser radiation,<sup>22</sup> and laser particle acceleration<sup>23,24</sup> in tenuous plasmas, benefit from a long interaction distance. In a homogeneous plasma the region of high intensity interaction is confined to approximately one Rayleigh diffraction length

$Z_R = k_0 r_0^2 / 2$ , where  $k_0$  is a laser wave number and  $r_0$  is a radius of focal spot. Propagation over longer distances requires some form of laser guiding. Guiding by a plasma channel is the most promising experimental approach<sup>25-29</sup> for high laser intensities. Excitation of relativistic plasma waves in channels was analyzed<sup>30-33</sup> for particle acceleration.

The guided laser pulses are not immune to parametric instabilities, such as forward and near-forward stimulated Raman scattering (SRS) in parabolic,<sup>16,34-39</sup> tapered,<sup>40</sup> leaky,<sup>41</sup> and single-mode flat channels,<sup>42</sup> or large-angle SRS in plasma-filled capillaries.<sup>43</sup> Commonly, the energy losses of a laser pulse and excessive plasma heating due to the large-angle SRS (including RBS) are undesirable for some applications,<sup>44</sup> and uncovering new physical mechanisms that enable the RBS suppression is up to date. For some applications, however, the RBS can be useful. For example, the laser pulse leading front depletion by the RBS may seed either forward SRS or resonant modulational instability.<sup>15,45</sup> Novel schemes of short-pulse amplification in a plasma<sup>18,19</sup> are based on the backscattering of a long moderately intense pump laser beam into a short counterpropagating signal pulse: the energy of the pump is absorbed by the signal as it is amplified and compressed. The Raman compression could be a viable path to obtaining high-power single-cycle pulses. For transversely homogeneous plasmas, one of the challenges of Raman amplification is to ensure the uniformity of plasma along the interaction axis so that the signal be downshifted from the pump by almost exactly the plasma frequency  $\omega_p$ . In the present paper we discover different features of the RBS in plasma channels, which are favorable for realization of Raman amplification (to anticipate, the RBS process in a deep plasma channel can be broadband enough to make exact resonant detuning of pump and signal unnecessary).

To enable analytic progress and to facilitate qualitative understanding, we focus on plasma channels that support a single confined high frequency (hf) EM mode, referred to as

<sup>a)</sup>Electronic mail: kalmykov@physics.utexas.edu

a fundamental mode of channel (FMC). The laser pulse confined in a channel is assumed to be the FMC. The RBS in a single-mode channel proceeds differently than in a homogeneous plasma and can be characterized by the following features: (a) reduction of the RBS peak temporal growth rate; (b) broadening of the RBS amplification bandwidth; and (c) modification of the transverse profile of scattered mode from that of FMC. Depending on the parameters of channel (such as on-axis plasma density and density depression) and pump laser (such as frequency and intensity), those modifications can be either more or less prominent.

It was suggested earlier<sup>42</sup> in the context of Raman forward scattering that variation of the plasma frequency across the channel may significantly reduce the peak growth rate. The effect occurs due to the strong localization of scattering electron plasma wave (EPW) near the channel axis. However, the complicated hybrid EM nature of a relativistic EPW in a channel<sup>30-33</sup> allowed for obtaining approximate results only.<sup>42</sup> Specifically, it was assumed that all the scattered radiation was in the fundamental channel mode. For the RBS, the EM component of the short-wavelength EPW may be neglected, enabling us to account for the modification of the transverse shape of the backscattered radiation beam. This is accomplished by expanding the transverse profile of the scattered field into the channel eigenmodes, i.e., the FMC plus continuum of the nonbound hf EM modes. These continuum modes of channel (CMC) do not exponentially decay outside of the channel (as the FMC does) and exhibit a cosinelike behavior at infinity, which makes them similar to the transverse Fourier harmonics of scattered radiation in a homogeneous plasma. The problem is complicated by the fact that the FMC and CMC are not independent in a channel. Radial shear of the plasma density couples them to each other, not only creating the field structure different from that of FMC but also affecting the spectrum of the instability. One of our goals is to evaluate the continuum-mode contribution to the RBS growth rate. We put emphasis on the regime of strong plasma wave localization (SPWL). Spectral features of this regime are markedly different from those of the homogeneous-plasma RBS. The SPWL occurs when the parameter  $\eta = (\Delta\omega_p/\omega_{p1})^2/(2\gamma_{\text{hom}}/\omega_{p1})$  is large compared to unity {here and elsewhere,  $\gamma_{\text{hom}} = \sqrt{|\mathbf{a}_0|^2\omega_0\omega_{p1}/4}$  is the maximum increment of the weakly coupled RBS in a homogeneous plasma,<sup>1,2</sup>  $\omega_{p1} = \omega_p(x=0)$  is a plasma frequency on axis,  $\Delta\omega_p^2$  is the channel depth, and  $\mathbf{a}_0 = e\mathbf{E}_0/(m_e\omega_0c)$  is a normalized amplitude of electric field of the pump wave}, which physically means that the plasma frequency depression in a channel exceeds the RBS bandwidth in a homogeneous plasma. In the SPWL regime, the maximum temporal increment is shown to scale as  $\gamma_{\text{hom}}/\sqrt[3]{\eta}$ . Hence, plasma wave localization suppresses the instability. On the other hand, the transverse shear of the plasma frequency results in a broader instability bandwidth. The spectral maximum of backscattered light is found to be redshifted from the pump frequency by more than  $\omega_{p1}$ , and the spectrum itself extends on the red side far beyond the frequency bandwidth of the homogeneous-plasma RBS. The bandwidth increase is due to the backscattering off the channel regions with higher local

plasma frequencies and, therefore, higher redshifts of scattered light. In the SPWL regime, the CMC contribution transversely shrinks the fastest-growing radiation mode. This effect enhances the RBS: in the numerical examples presented in the paper, the continuum modes add from 25% to 50% to the peak value of temporal increment.

The CMC contribution to the RBS process may be neglected if the pump amplitude is sufficiently small (or the channel is deep) to satisfy the inequality  $u_0 \ll (\Delta\omega_p/\omega_{p1})^2/(\omega_0/\omega_{p1})^{5/4}$ . This regime is referred to as single mode, because all the scattered field is concentrated now in the FMC. The nonlinear interaction of two bound EM modes through a localized EPW allows us to consider the single-mode RBS as a channel analog of the three-wave (i.e., weakly coupled) RBS in a homogeneous plasma (however, these three-wave parametric processes have vastly different spectral properties). The evolution of a single-mode backscattered EM signal in the field of a single-mode pump is described analytically by solving the initial-value problem. In the single-mode regime, the maximum of the signal moves with the velocity  $2c/3$ , which is higher than a group velocity of scattered radiation  $c/2$  in the weakly coupled RBS in a homogeneous plasma. High group velocity of the amplified pulse and its broad bandwidth produced by the transverse shear of plasma density profitably distinguish the single-mode Raman amplification in a plasma channel from its homogeneous-plasma counterpart.<sup>19</sup>

The paper is organized as follows. In Sec. II the single-mode plane plasma channel is introduced, and basic equations governing the nonlinear plasma response to the combined pump and scattered radiation are derived. These equations are solved in Sec. III by the mode expansion, and the generalized dispersion relation is derived. This dispersion relation allows for the coupling between the FMC and CMC of scattered radiation. In Sec. IV, the dispersion equation is solved in the most interesting and novel regime of SPWL. The range of parameters where the CMC contribution to the RBS process is negligible is found. The spectral bandwidth and peak temporal growth rate of the single-mode regime are evaluated. In Sec. V the initial-value problem describing the linear evolution of the EM signal is formulated and solved, and the group velocity of the signal is calculated. Summary of the results is given in Sec. VI. The Appendix reviews some properties of the associated Legendre functions with an imaginary order which describe the continuum of EM channel eigenmodes.

## II. BASIC EQUATIONS

To begin with, we define the unperturbed state of plasma and laser radiation, that is, the background on which the instability grows. In order to make an analytic progress, a plane plasma channel is chosen with the density profile

$$\omega_p^2(x) = \omega_{p2}^2 - (\Delta\omega_p^2/2)\cosh^{-2}(x/\sigma). \quad (1)$$

Plasma frequency in the channel varies between  $\omega_{p1} = (\omega_{p2}^2 - \Delta\omega_p^2/2)^{1/2}$  at the center and  $\omega_{p2}$  at infinity. Relative plasma density depression is  $n_e(x=0)/n_e(|x|=\infty) = (1 + \Delta\omega_p^2/2)^{-1}$ , where  $\Delta\omega_p = \Delta\omega_p/\omega_{p1}$ . Throughout the rest of the paper,

electron density at the channel axis is held fixed and the channel depth is varied. The normalized hf electric field of pump radiation with an arbitrary polarization is

$$\tilde{\mathbf{a}}_0(x, z, t) = \text{Re}[\mathbf{a}_0(x)e^{ik_0z - i\omega_0 t}]. \quad (2)$$

The amplitude of laser electric field in the channel is the solution of the eigenvalue problem

$$\mathcal{L}_0 \mathbf{a}_0 \equiv [-\partial^2/\partial x^2 + k_p^2(x)] \mathbf{a}_0 = \lambda_0 \mathbf{a}_0 \quad (3)$$

with the boundary condition  $a_0(|x| \rightarrow \infty) \rightarrow 0$  [here,  $\lambda_0 \equiv (\omega_0/c)^2 - k_0^2$ ,  $k_p(x) \equiv \omega_p(x)/c$ , and  $a_0 = |\mathbf{a}_0|$ ]. In Eq. (3), we assume  $k_{p1}\sigma \sim \mathcal{O}(1)$ ,  $k_{p1} = \omega_{p1}/c$ , and  $a_0 \ll 1$ , and neglect a relativistic correction to the mass of electron oscillating in the pump field. Thus, relativistic self-focusing of a laser beam<sup>46</sup> is excluded. Relativistic self-guiding effects will be addressed in future publications. We require that the eigenvalue problem (3) has the unique solution decaying at  $|x| \rightarrow \infty$ , which gives the transverse profile of the FMC,

$$a_0(x) = u_0 \cosh^{-1}(x/\sigma) \equiv u_0 \psi_0, \quad (4)$$

and a relation between the plasma channel depth and width,

$$\Delta \omega_p \sigma / c = 2. \quad (5)$$

Also, the eigenvalue equation gives the dispersion relation for the pump field,

$$\lambda_0 = \omega_0^2/c^2 - k_0^2 = k_{p2}^2 - \sigma^{-2}, \quad (6)$$

where  $k_{p2} = \omega_{p2}/c$ .

The perturbed hf electric field in a plasma is

$$\tilde{\mathbf{a}}(x, z, t) = \tilde{\mathbf{a}}_0 + \text{Re}[\mathbf{a}_s(x, z, t)e^{-i\omega_s t + ik_s z}], \quad (7)$$

where  $\mathbf{a}_s = e\mathbf{E}_s/(m_e \omega_0 c)$  ( $|\mathbf{a}_s| \ll a_0$ ) is a complex amplitude of the normalized electric field of backscattered radiation,  $\omega_s = \omega_0 - \omega_{p1}$ , and  $k_s = -k_0 + k_{p1}$ . In the case of rarefied plasma ( $\omega_p \ll \omega_0$ ), which is considered here, the RBS is a resonant process<sup>2</sup> in which only the Stokes component of scattered radiation is involved [see Eq. (7)]. The amplitudes  $a_{0(s)}$  are slowly varying in time and space on the scales  $\omega_0^{-1}$  and  $k_0^{-1}$ , respectively. We shall consider the weakly coupled RBS (Refs. 1 and 2), whose temporal increment is smaller than the electron Langmuir frequency (which is valid at  $u_0 < \sqrt{\omega_p/\omega_0}$ ). Hence, the envelope of scattered radiation is slowly varying in time and in the direction of propagation,  $z$ :  $|\partial a_s/\partial t| \ll \omega_{p1}|a_s|$ ,  $|\partial a_s/\partial z| \ll k_{p1}|a_s|$ .

We neglect the ion density perturbation produced by the laser and scattered radiation. We consider ions to be a fixed neutralizing positive background in the form of a channel with a density profile given by Eq. (1). This assumption is adequate for laser pulses shorter than an ion plasma period ( $\tau_L \ll 2\pi\omega_{pi}^{-1}$ ). In the opposite limit of long pulses, various parametric instabilities have been analyzed previously.<sup>35</sup> Ponderomotive force due to the interference of incident and scattered radiation excites perturbations of electron density,  $\delta \tilde{n}_e = n_e - n_0(x)$ ,

$$\delta \tilde{n}_e(x, z, t) = \text{Re}[\delta n_e(x, z, t)e^{-i\omega_{p1} t + ik_e z}], \quad (8)$$

where  $k_e = k_0 - k_s$ . In rarefied plasmas, the amplitude  $\delta n_e$  of the scattering EPW varies in space slowly on the scale  $k_0^{-1}$ .

Moreover, for the regime of weak coupling, this amplitude is slowly varying on plasma temporal and spatial periods:  $|\partial \delta n_e/\partial t| \ll \omega_{p1}|\delta n_e|$ ,  $|\partial \delta n_e/\partial z| \ll k_{p1}|\delta n_e|$ .

The amplitudes of scattered EM wave and scattering EPW obey the coupled-mode equations, which follow from the equations of nonrelativistic hydrodynamics of electron fluid in the hf EM field (7) and Maxwell's equations for the scattered radiation,

$$\left[ \frac{\partial}{\partial t} - c \frac{\partial}{\partial z} + i \frac{c^2}{2\omega_s} (\mathcal{L}_0 - \lambda_s) \right] a_s = \omega_{p1} G_1 \psi_0 \nu, \quad (9a)$$

$$\left[ \frac{\partial}{\partial t} - i\omega_{p1} \left( \frac{\Delta \bar{\omega}_p}{2} \right)^2 (1 - \psi_0^2) \right] \nu = \omega_{p1} G_2 \psi_0 a_s, \quad (9b)$$

where  $\nu = \bar{\omega}_p^2 [\delta n_e^*/n_0(x)]$ ,  $G_1 = u_0/(4i\bar{\omega}_s)$ ,  $G_2(x) = i\bar{\omega}_0^2 \bar{\omega}_p^2 u_0$  with  $\bar{\omega}_{0,s} = \omega_{0,s}/\omega_{p1}$ ,  $\bar{\omega}_p = \omega_p(x)/\omega_{p1}$ , and  $\lambda_s = (\omega_s/c)^2 - k_s^2$ . The difference between  $\lambda_s$  and  $\lambda_0$  is eliminated from all the further equations by the substitution  $a_s, \nu \propto \exp[ic z(\lambda_0 - \lambda_s)/(2\omega_s)]$ . The set (9) is valid under assumption that the short-wavelength scattering EPW ( $k \approx 2k_0 \gg k_{p2}$ ) is predominantly electrostatic, and its EM component is neglected.<sup>42</sup> This assumption will be validated in Sec. III. We scale time and space to  $\omega_{p1}^{-1}$  and  $k_{p1}^{-1}$ , respectively, and introduce the dimensionless variables  $\bar{t} = \omega_{p1} t$ ,  $\{\bar{z}, \bar{x}\} = k_{p1}\{z, x\}$  (all the overbarred quantities which appear in formulas below are normalized in this way). Equations (9) recast now as

$$\left[ \frac{\partial}{\partial \bar{t}} - \frac{\partial}{\partial \bar{z}} + \frac{i}{2\bar{\omega}_s} (\bar{\mathcal{L}}_0 - \bar{\lambda}_0) \right] a_s = G_1 \psi_0 \nu, \quad (10a)$$

$$\left[ \frac{\partial}{\partial \bar{t}} - i \left( \frac{\Delta \bar{\omega}_p}{2} \right)^2 (1 - \psi_0^2) \right] \nu = G_2 \psi_0 a_s. \quad (10b)$$

In Sec. III, we derive from Eqs. (10) the dispersion relation of RBS in the channel (1).

### III. GENERAL DISPERSION RELATION

Equations (10) can be solved by using the Fourier–Laplace transform of the envelopes,  $a_s, \nu \propto \exp(i\bar{\omega}\bar{t} - i\bar{k}\bar{z})$ . It is convenient to introduce a new variable  $y = \tanh(x/\sigma)$  and express  $\psi_0 = \sqrt{1 - y^2}$  and  $\bar{\omega}_p^2 = 1 + C^2 y^2$ , where  $C^2 = \Delta \bar{\omega}_p^2/2 = 2/\bar{\sigma}^2$ . Plasma occupies the area  $-1 < y < 1$ . Expressing  $\nu$  through  $a_s$  from Eq. (10b), plugging it to Eq. (10a), and using Eqs. (5) and (6), we obtain the equation for  $a_s(y, \bar{k}, \bar{\omega})$ ,

$$\mathcal{L}_{1,1} a_s = \bar{\sigma}^2 \left( \frac{p^2}{1 - y^2} + \frac{G}{\bar{\omega}} \mathcal{G}(\bar{\omega}, y) \right) a_s, \quad (11)$$

where  $p^2 = 2\bar{\omega}_s(\bar{\omega} + \bar{k})$ ,  $G = u_0^2 \bar{\omega}_0^2/2$ ,  $\mathcal{G}(\bar{\omega}, y) = (1 + C^2 y^2)/(1 - B^2 y^2)$ , and  $B^2 = \Delta \bar{\omega}_p^2/(4\bar{\omega}) = (\bar{\sigma}^2 \bar{\omega})^{-1}$ . The function  $p^2(\bar{k})$  contains the information about propagation of scattered radiation. The operator in the left-hand side of Eq. (11) comes from the equation for the associated Legendre functions,<sup>47</sup>

$$\mathcal{L}_{\mu,s} P_s^\mu(y) \equiv \left\{ \frac{d}{dy}(1-y^2) \frac{d}{dy} + s(s+1) - \frac{\mu^2}{1-y^2} \right\} P_s^\mu(y) = 0 \tag{12}$$

with  $s=\mu=1$ . Given the degree  $s=1$ , the spectrum of Eq. (12) consists of one discrete level with  $\mu=1$  and a continuum of modes with  $\mu^2=-q^2$ ,  $q$  real. Hence, the full set of solutions of Eq. (11) is composed of the single FMC  $P_1^1(y)=\psi_0$  and the set of CMC,

$$P_1^{\pm iq}(y) = \frac{\tanh(x/\sigma) \mp iq}{(1 \mp iq)\Gamma(1 \mp iq)} e^{\pm iq x/\sigma} = \frac{1}{\Gamma(1 \mp iq)} \frac{y \mp iq}{1 \mp iq} \left( \frac{1+y}{1-y} \right)^{\pm iq/2} \tag{13}$$

At  $|x| \rightarrow \infty$ , the CMC (13) reveal the cosinelike behavior [see Eqs. (A2)]. Unlike the pump field given in the form of FMC, the scattered radiation in a channel is not necessarily represented solely by FMC. The CMC (13) describe the discrepancy between the true profile of EM field and the FMC. Therefore, we express the general solution of Eq. (11) as a mode expansion,

$$a_s(y) = P_1^1(y) + \int_{-\infty}^{+\infty} P_1^{iq}(y) a_s(q) dq \tag{14}$$

Knowing that  $\mathcal{L}_{1,1} P_1^1 = 0$  and  $\mathcal{L}_{1,1} P_1^{iq}(y) = -(1+q^2)(1-y^2)^{-1} P_1^{iq}(y)$ , we arrive at the following equation:

$$\int_{-\infty}^{+\infty} P_1^{iq}(y) \frac{1+q^2}{1-y^2} a_s(q) dq = -\bar{\sigma}^2 \left( \frac{p^2}{1-y^2} + \frac{G}{\bar{\omega}} \mathcal{G}(\bar{\omega}, y) \right) \times \left( P_1^1(y) + \int_{-\infty}^{+\infty} P_1^{iq}(y) a_s(q) dq \right) \tag{15}$$

We multiply Eq. (15) by  $P_1^1(y)$  and integrate it over  $y$ . Having in mind that  $\int_{-1}^1 P_1^{iq}(y) (1-y^2)^{-1/2} dy = 0$  [formula (7.132.1) of Ref. 47], we arrive at the dispersion equation

$$p^2 + \frac{G}{2\bar{\omega}} \tilde{Q}(\bar{\omega}) = -\frac{G}{2\bar{\omega}} \int_{-\infty}^{+\infty} F(\bar{\omega}, q) a_s(q) dq, \tag{16}$$

where

$$F(\bar{\omega}, iq) = \int_{-1}^1 \mathcal{G}(\bar{\omega}, y) (1-y^2)^{1/2} P_1^{iq}(y) dy, \tag{17}$$

and the plasma response function is

$$\begin{aligned} \tilde{Q}(\bar{\omega}) &= \int_{-1}^1 (1-y^2) \mathcal{G}(\bar{\omega}, y) dy \\ &= \frac{2}{B^2} \left( 1 - \frac{2C^2}{3} + \frac{C^2}{B^2} \right) \\ &\quad - \frac{(B^2 + C^2)(1-B^2)}{B^5} \ln \left( \frac{1+B}{1-B} \right). \end{aligned} \tag{18}$$

It has been shown previously<sup>42</sup> that the function (18) de-

scribes a purely electrostatic response of plasma in the limit of a broad shallow channel, that is,  $k_e \sigma \gg 1$ . In the case of RBS  $k_e \approx 2k_0$ . Thus, any channel with  $\sigma > k_0^{-1}$  is wide, and the electrostatic description is always applicable to the plasma response in the RBS process.

In order to find a closed-form dispersion equation we have to determine explicitly the CMC amplitudes  $a_s(q)$  in Eq. (16). We multiply Eq. (15) by  $P_1^{-iq}(y)$  and integrate it over  $y$ . Using the orthogonality condition (A1) and the identity  $\Gamma(1+iq)\Gamma(1-iq) = \pi q / \sinh(\pi q)$ ,<sup>47</sup> we obtain the expres-

$$a_s(q) = -\bar{\sigma}^2 \left( \frac{G}{2\bar{\omega}} \right) \frac{q/\sinh(\pi q)}{1 + (\bar{\sigma}p)^2 + q^2} \times \left( F(\bar{\omega}, -iq) + \int_{-\infty}^{+\infty} F_1(\bar{\omega}, q, q') a_s(q) dq \right), \tag{19}$$

where the kernel  $F_1 = \int_{-1}^1 \mathcal{G}(\bar{\omega}, y) P_1^{iq}(y) P_1^{-iq'}(y) dy$  describes the coupling between the modes of continuum with different indices  $q$ . Further, we take into account only the coupling between the FMC and CMC, and set  $F_1(\bar{\omega}, q, q') \equiv 0$ . The resulting dispersion relation is

$$p^2 + \frac{G}{2\bar{\omega}} \tilde{Q}(\bar{\omega}) = \bar{\sigma}^2 \left( \frac{G}{2\bar{\omega}} \right)^2 \Phi(\bar{\omega}, p), \tag{20a}$$

$$\Phi(\bar{\omega}, p) = \int_{-\infty}^{+\infty} \frac{F(\bar{\omega}, iq) F(\bar{\omega}, -iq)}{1 + (\bar{\sigma}p)^2 + q^2} \frac{q dq}{\sinh(\pi q)}. \tag{20b}$$

Equation (20a) describes the spatiotemporal evolution of initial perturbations of field and electron density.<sup>48</sup> Real and imaginary parts of the complex frequency  $\bar{\omega}$  as a function of real wave number shift  $\bar{k}$  determine the temporal evolution of spatial Fourier harmonics of the signal, and can be used to solve the initial-value problem. In the following section, the complex solution  $\bar{\omega}(\bar{k})$  (with  $\bar{k}$  real) of the dispersion equation (20a) will be found in the limit of SPWL. The SPWL is achieved when the channel depth  $\Delta \bar{\omega}_p^2$  is much larger than the instability bandwidth, i.e.,  $\Delta \bar{\omega}_p^2 \gg |\bar{\omega}|$ , or  $|B|^2 \gg 1$ . The unstable EPW will be found confined in the near-axis area with a transverse extent of about  $|B|^{-1}$ . For this regime, the contribution from CMC to the growth rate can be important.

#### IV. SOLUTION OF DISPERSION RELATION IN THE SPWL REGIME

##### A. Temporal increment of instability

The range of parameters for the SPWL regime is prescribed by the inequality  $|B|^2 > 1$ , or  $|\bar{\omega}| < (\Delta \bar{\omega}_p/2)^2$ . Taking the estimate  $|\bar{\omega}| \sim \bar{\gamma}_{\text{hom}} = (u_0/2) \sqrt{\bar{\omega}_0}$ , we establish the limitation on the laser amplitude,

$$u_0 < U_0 \equiv \Delta \bar{\omega}_p^2 / (2\sqrt{\bar{\omega}_0}). \tag{21}$$

Equation (21) provides the same scaling in  $\bar{\omega}_0$  as the condition of weak coupling  $u_0 < 1/\sqrt{\bar{\omega}_0}$  for the RBS in homogeneous plasmas.<sup>2</sup> The condition  $|B|^2 > 1$  has an important physical consequence: the unstable electron density perturba-

tions become localized stronger than the EM waves (the size of localization area is  $\delta\bar{x} \sim \bar{\sigma}/|B|$ ).

To evaluate the right-hand side (RHS) of dispersion equation (20a) in the limit  $|B|^2 \gg 1$ , we note that the integral (17) that determines the kernel of Eq. (20b) can be represented as  $F(\bar{\omega}, iq) = \int_{-1}^1 \mathcal{F}(y, iq) (1 - B^2 y^2)^{-1} dy$ , where  $\mathcal{F}(y, iq) = (1 + C^2 y^2) P_1^1(y) P_1^q(y)$  is independent of  $B$ . At  $|B|^2 \gg 1$ , only  $y$  values from the close vicinity of channel axis, that is,  $|y| < |B|^{-1}$ , will contribute to the integral. Therefore, effective coupling between the FMC and CMC occurs near the channel axis in the area with a transverse extent of order  $|B|^{-1}$ . In this case, the RHS of Eq. (20a) can be expanded in powers of  $B^{-1}$ . To evaluate the lowest-order term of the expansion, the on-axis value of  $\mathcal{F}(y, iq)$  is taken, i.e.,  $\mathcal{F}(0, iq) = -iq / [(1 - iq)\Gamma(1 - iq)]$ . Then, the integral (20b) becomes

$$\begin{aligned} \Phi &\approx \frac{1}{\pi} \left( \int_{-1}^1 \frac{dy}{1 - B^2 y^2} \right)^2 \int_{-\infty}^{+\infty} \frac{(1 + q^2)^{-1} q^2 dq}{[1 + (\bar{\sigma}p)^2 + q^2]} \\ &= \frac{\sqrt{1 + (\bar{\sigma}p)^2} - 1}{(\bar{\sigma}Bp)^2} \ln^2 \left( \frac{1 + B}{1 - B} \right) \approx \frac{1 - \sqrt{1 + (\bar{\sigma}p)^2}}{\pi^2 (\bar{\sigma}Bp)^2}. \end{aligned} \quad (22)$$

Evaluating the plasma response function in the limit of large  $|B|$  as  $\tilde{Q}(\bar{\omega}) \approx i\pi/B$ , we reduce Eq. (20a) to a relatively simple form:

$$p^2 + \frac{G}{2\bar{\omega}} \frac{i\pi}{B} = \left( \frac{G}{2\bar{\omega}} \right)^2 \left( \frac{\pi}{Bp} \right)^2 [1 - \sqrt{1 + (\bar{\sigma}p)^2}]. \quad (23)$$

It is now evident that the CMC cannot be *a priori* excluded from the process of RBS with SPWL. Depending on whether the CMC contribution [that is, the RHS of the dispersion relation (23)] can or cannot be neglected, the RBS with SPWL proceeds in single-mode or multimode subregime. Spectral features of these subregimes we specify below.

Under the condition  $|\bar{\sigma}p|^2 \sim 2\bar{\omega}_0/|B|^2 < 1$ , the CMC contribution may be eliminated from Eq. (23):

$$p^2 + [G/(2\bar{\omega})](i\pi/B) = 0. \quad (24)$$

Equation (24) describes the interaction of two EM waves (pump and scattered, FMC both), via strongly localized EPW. This three-wave interaction is a channel counterpart of the three-wave RBS in a homogeneous plasma (these processes, however, have quite different spectral properties). Equation (24) yields the solution with a maximum imaginary part,

$$\bar{\omega}(\bar{k} = 0) = e^{i\pi/3} \sqrt[3]{\pi^2/(2\eta)} \bar{\gamma}_{\text{hom}}, \quad (25)$$

where the parameter  $\eta = \Delta\bar{\omega}_p^2/(2\bar{\gamma}_{\text{hom}}) > 1$  is of the order of  $|B|^2$ . Real part of the solution (25) gives the redshift of spectral maximum  $\Delta\bar{\omega} = \sqrt[3]{\pi^2/(2\eta)} (\bar{\gamma}_{\text{hom}}/2)$ . Equation (24) also predicts a blue-side limitation of the RBS bandwidth at  $\text{Re}\bar{\omega}_c = -\sqrt[3]{\pi^2/\eta} (\bar{\gamma}_{\text{hom}}/2)$ . From the red side ( $\text{Re}\bar{\omega} > 0$ ), Eq. (24) gives no limitation, and the spectrum has a tail far extended in this area.

The validity condition  $|B|^2 > 2\bar{\omega}_0 \gg 1$  for Eq. (24) puts the border between the SPWL subregimes. It is more restrictive than  $|B|^2 > 1$  and may be written as  $|\bar{\omega}| < \Delta\bar{\omega}_p^2/(8\bar{\omega}_0)$ . Substituting the solution (25) into the latter inequality provides the range of parameters for the single-mode subregime:

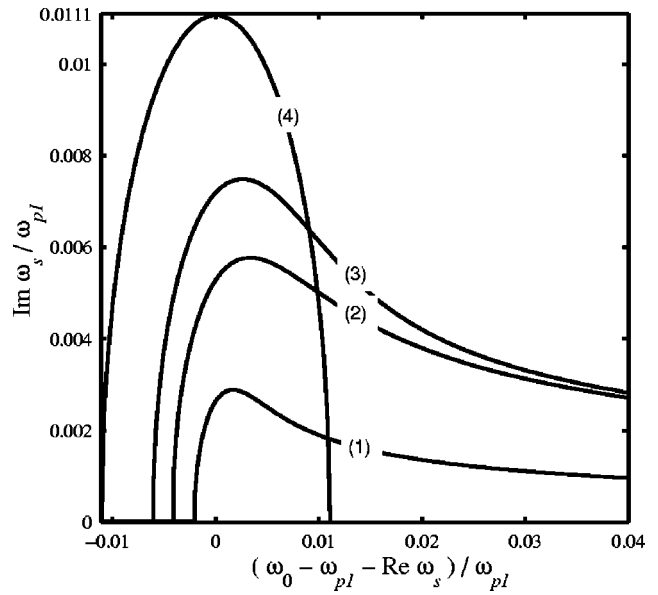


FIG. 1. Spectra of RBS in the regime of strong plasma wave localization. Normalized increment is plotted against the real part of frequency. Laser and plasma parameters are  $\bar{\omega}_0 = 10$  and  $u_0 \approx 0.007$ . Plasma frequency depression in a channel is (I)  $\Delta\bar{\omega}_p = 2$  [curve (1)] and (II)  $\Delta\bar{\omega}_p = 1/\sqrt{2}$  [curves (2) and (3)]. The line (4) is a reference spectrum corresponding to the homogeneous plasma ( $\bar{\omega}_p \equiv 1$ ). The inhomogeneity of  $\omega_p(x)$  redshifts the spectral maxima and creates the tails on the red side.

$$u_0 < U_1 \equiv U_0 [\sqrt{\pi} (2\bar{\omega}_0)^{3/4}] \ll U_0. \quad (26)$$

The larger  $u_0$ , the stronger the instability is driven and the larger is the population of CMC excited. When  $u_0$  falls within the interval

$$U_1 < u_0 < U_0, \quad (27)$$

the CMC contribution is no more negligible and the RBS process becomes essentially multimode. The dispersion equation (23), whose RHS cannot be omitted now, is solved numerically.

In Fig. 1, we present an example of the dispersion curves obtained for the RBS in both single-mode and multimode SPWL regimes. For the fixed values of normalized laser frequency  $\bar{\omega}_0 = 10$  and amplitude of electric field  $u_0 = 0.007$ , the increment  $\text{Im}\bar{\omega}$  is found numerically versus  $\text{Re}\bar{\omega}$  for the two different values of channel depth: (I)  $\Delta\bar{\omega}_p = 2$ , or  $n_e(x=0)/n_e(|x|=\infty) = 1/3$ , and (II)  $\Delta\bar{\omega}_p = 1/\sqrt{2}$ , or  $n_e(x=0)/n_e(|x|=\infty) = 0.8$ . In Fig. 1, the solution of Eq. (23) for the set of parameters (I) is plotted with the curve (1). The curves (2) and (3) are the solutions of the same equation for the set of parameters (II), with the CMC contribution deducted in the case of curve (2). The curve (4) is a reference spectrum of RBS in a homogeneous plasma ( $\bar{\omega}_p \equiv 1$ ).

Parameter sets (I) and (II) correspond to the SPWL regime as the condition  $u_0 \ll U_0$  is very well satisfied for both. For the set (I) the inequality  $u_0 < U_1 \approx 0.019$  holds, and the single-mode regime is the case. Contribution from the CMC is negligibly small: numerical solutions of the full [Eq. (23)] and single-mode [Eq. (24)] dispersion equations coincide within a thickness of the line (1). Such a good coincidence is not the case for the parameter set (II), which corresponds to

the multimode regime ( $u_0 > U_1 \approx 0.0047$ ). Comparison between the curves (2) and (3) demonstrates considerable enhancement of RBS due to the CMC contribution: the increase in the peak increment amounts to about 25%. The basic characteristics of RBS in the multimode SPWL regime can be summarized as follows.

- (1) The peak growth rate is reduced if compared with the case of homogeneous plasma.
- (2) Contribution from the CMC enhances the scattering process.
- (3) The RBS bandwidth inside a channel is significantly larger than in a homogeneous plasma.
- (4) The frequency spectrum experiences overall redshift from the Stokes frequency  $\omega_0 - \omega_{p1}$ .

The last two features are clear advantages of the SPWL regime for the Raman amplification of short pulses in plasmas.<sup>19</sup> Due to the broadband nature of the process, exact tuning the signal frequency to  $\omega_0 - \omega_{p1}$  is not necessary to get a considerable amplification rate in the linear regime. We can also estimate the RBS growth rate modification for the parameters typical of a channel-guided laser driven accelerator. The plasma channel created in the experiment<sup>29</sup> was capable of single-mode guiding of the laser pulse with a radius  $8 \mu\text{m}$  at the level  $e^{-2}$  in intensity, which under ansatz (4) gives  $\sigma = 4.65 \mu\text{m}$ . The electron density  $4 \times 10^{18} \text{cm}^{-3}$  at the bottom of the channel gives  $k_{p1}\sigma = 1.75$  and, according to the matching condition (5), provides the reduction of normalized electron density  $\Delta\bar{\omega}_p^2 \approx 1.3$ , which corresponds to the effective density depression by a factor 0.6. The laser wavelength  $0.8 \mu\text{m}$  gives  $\bar{\omega}_0 \approx 21$ . To comply with the limitation  $u_0 < U_0 \approx 0.14$  [see Eq. (21)] the intensity of guided laser must be lower than  $4 \times 10^{16} \text{W/cm}^2$ . For  $I \approx 4 \times 10^{14} \text{W/cm}^2$  ( $u_0 \approx 0.0136$ ,  $\gamma_{\text{hom}} \approx 0.031\omega_{p1}$ ) RBS proceeds in the multimode SPWL regime with  $\eta \approx 21$ . The peak increment roughly evaluated from Eq. (25) is  $\gamma \approx 0.54\gamma_{\text{hom}}$ ; adding the CMC contribution increases it up to  $0.89\gamma_{\text{hom}}$ . Therefore, in the regime considered, 11% reduction of the peak RBS increment can be expected in comparison with the case of homogeneous plasma, and the CMC add to the peak increment about 40% of its value.

### B. Transverse profile of scattered radiation in the multimode SPWL regime

Results of Sec. IV A show high sensitivity of the RBS to the transverse structure of scattered radiation beam in a channel: contribution from the CMC increases the growth rate. We find here the CMC-related correction to the transverse profile of the beam. For the parameter set (II) [the curve (3) in Fig. 1] we evaluate the integral (14) numerically for the fastest growing mode and present the distributions of intensity  $|a_s(\bar{x})|^2$  in Fig. 2. The solid curve is given by Eq. (14). The intensity profile of FMC is provided for reference and plotted with a dashed line. Figure 2 shows the reduction of beam width and increase in the on-axis intensity produced by coupling between the FMC and CMC. Reduction of the rms beam size amounts to  $(\langle \bar{x}_{\text{FMC+CMC}}^2 \rangle / \langle \bar{x}_{\text{FMC}}^2 \rangle)^{1/2} \approx 0.77$ , where  $\langle \bar{x}^2 \rangle^{1/2} = [\int_{-\infty}^{+\infty} \bar{x}^2 |a_s(\bar{x})|^2 d\bar{x} / \int_{-\infty}^{+\infty} |a_s(\bar{x})|^2 d\bar{x}]^{1/2}$ . Although 23%

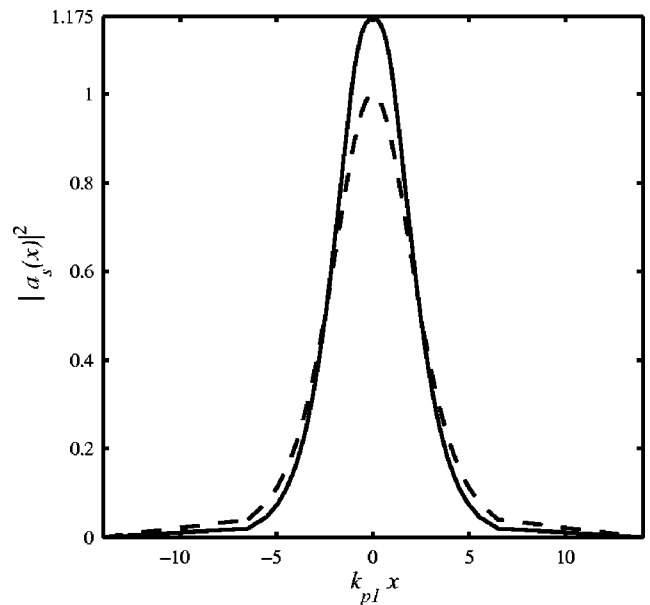


FIG. 2. Transverse profile of intensity for the fastest growing spectral component of scattered radiation (solid line) numerically evaluated from Eq. (14) for the parameter set (II) of Fig. 1, complex frequency given by the maximum of the curve (3). The dashed line is the intensity profile of FMC. The CMC contribution shrinks the radiation beam and increases the field near the channel axis.

compression of the intensity profile occurs for the parameters chosen, the power of scattered radiation remains almost unchanged: difference between the integrals  $\int_{-\infty}^{+\infty} |a_s(\bar{x})|^2 d\bar{x}$  calculated for the FMC and FMC+CMC is about 3%. For the estimates made at the end of Sec. IV A, the compression and intensity enhancement on the axis amount to about 28% and 40%, respectively. Hence, in the multimode SPWL regime, coupling between the FMC and CMC shrinks the scattered radiation near channel axis where the pump field has the maximum. As a consequence, increase in the peak increment occurs.

## V. SPATIOTEMPORAL EVOLUTION OF BACKSCATTERED SIGNAL IN THE SINGLE-MODE SPWL REGIME

### A. Group velocity of scattered radiation

In this section we address the linear Raman amplification of EM wave packet in a plasma channel. First, we evaluate the group velocity of backscattered signal, i.e.,  $v_g \equiv \partial \text{Re}\omega / \partial k$  at  $\partial \text{Im}\omega / \partial k = 0$ . By definition, thus calculated group velocity determines the speed of the signal peak. On substituting  $\bar{\omega} = \Omega + i\gamma$  (with  $\Omega$  and  $\gamma$  real) into the dispersion relation (24), we separate real and imaginary parts of the equation, exclude  $\gamma$ , and obtain the algebraic relation which defines implicitly the dispersion function  $\Omega(\bar{k})$ :

$$\bar{k}^2 + 4\bar{k}\Omega + 3\Omega^2 - \frac{\Omega^3 + 2\bar{k}\Omega^2 + \bar{k}^2\Omega + b}{3\Omega + 2\bar{k}} = 0, \quad (28)$$

where  $b = \pi G / (2\sqrt{2}\bar{\omega}_0\Delta\bar{\omega}_p)$ . Differentiating Eq. (28) with respect to  $\bar{k}$  and plugging to the resulting equation  $\bar{k} = 0$  and  $\Omega(0) = \text{Re}\bar{\omega}$  from Eq. (25) (i.e., the wave number and real

part of frequency corresponding to the peak growth rate), we find the group velocity  $v_g = -2c/3$  (the minus sign means that the amplified pulse moves in the backward direction).

The absolute value of the group velocity in a channel is higher than in a homogeneous plasma, where  $v_{g\text{hom}} = -c/2$ . To get a qualitative interpretation of this effect we return to the basic equations (10). Taking the single-mode approximation for the envelope  $a_s(\bar{x}, \bar{z}, \bar{t}) \approx A_s(\bar{z}, \bar{t})\psi_0(\bar{x})$ , initial condition  $\nu(\bar{t}=0) \equiv 0$ , and the plasma response function  $\tilde{Q}(\bar{\omega}) \approx \pi i/B(\bar{\omega}) = (2\pi/\Delta\bar{\omega}_p)\sqrt{i\bar{\omega}}$ , we reduce the set (10) to the single equation  $(\partial_{\bar{t}} - \partial_{\bar{z}})A_s \approx u_0[\Delta\bar{\omega}_p/(16\bar{\omega}_0)]\langle N(\bar{t}) \rangle$ , where the overlap integral  $\langle N(\bar{t}) \rangle \equiv \int_{-\infty}^{+\infty} \psi_0^2(\delta n_e^*/n_0)dx$  between the profiles of electron density perturbation and pump field is evaluated as  $\langle N(\bar{t}) \rangle = u_0\sqrt{\pi i}(2\bar{\omega}_0/\Delta\bar{\omega}_p)^2 \int_0^{\bar{t}} A_s(\tau)/\sqrt{\bar{t}-\tau}d\tau$ . Obviously, the transverse shear of plasma density produces an effective decay of the plasma response expressed in terms of the convolution  $\langle N(\bar{t}) \rangle \propto A_s(\bar{t}) * \bar{t}^{-1/2}$  [compare with the non-damped case of homogeneous plasma, where  $(\partial_{\bar{t}} - \partial_{\bar{z}})a_s = \bar{\gamma}_{\text{hom}}^2 \int_0^{\bar{t}} a_s(\tau)d\tau \equiv \bar{\gamma}_{\text{hom}}^2 a_s(\bar{t}) * 1$ ]. Therefore, the tail of the amplified signal experiences the reduction of growth rate according to  $A_s(\bar{t}) \propto \langle N(\bar{t}) \rangle \propto A_s(\bar{t}) * \bar{t}^{-1/2}$ , and, consequently, the signal maximum moves closer to the signal leading front than in a homogeneous-plasma case. This argument qualitatively explains the increase in the group velocity of scattered light in a channel.

**B. Evolution of EM wave packet**

We solve here the initial-value problem for Eqs. (10),  $\bar{\nu}(\bar{t}=0) \equiv 0$ ,  $a_s(\bar{x}, \bar{z}, \bar{t}=0) = a_{s0}(\bar{z})\psi_0(\bar{x})$ , which specifies the EM wave packet initially matched with an unperturbed plasma channel. We naturally take account of these initial conditions by introducing a new dependent variable  $a_s^\dagger(\bar{x}, \bar{z}, \bar{t}) = a_s(\bar{x}, \bar{z}, \bar{t})H(\bar{t})$  [where  $H(\bar{t})$  is the Heaviside step function]. In the characteristic variables  $\theta = -\bar{z}$  and  $\eta = -\bar{z} - \bar{t}$ , the set (10) reads

$$\left[ \frac{\partial}{\partial \theta} + \frac{i}{2\bar{\omega}_s}(\bar{\mathcal{L}}_0 - \bar{\lambda}_0) \right] a_s^\dagger - G_1 \psi_0 \nu = a_{s0}(-\theta) \psi_0 \delta(\theta - \eta),$$

$$\left[ \frac{\partial}{\partial \eta} - \frac{\Delta\bar{\omega}_p^2}{4i}(1 - \psi_0^2) \right] \nu + G_2 \psi_0 a_s^\dagger = 0,$$

where  $\delta(t)$  is the Dirac delta function. We apply the Fourier transform with respect to the comoving ‘‘spatial’’ variable  $\eta$ , assuming  $\delta(\theta - \eta) = (2\pi)^{-1} \int_{-\infty}^{+\infty} \exp[ik(\eta - \theta)]dk$ , and then exclude the Fourier image  $\nu(\bar{x}, \theta, k)$ . Multiplying the resulting equation for the Fourier image  $a_s^\dagger(\bar{x}, \theta, k)$  by  $\psi_0(\bar{x})$  and then integrating it over  $\bar{x}$  gives the averaged equation

$$\left\{ \left\langle \psi_0 \frac{\partial a_s^\dagger}{\partial \theta} \right\rangle + \frac{i}{2\bar{\omega}_s} \left\langle \psi_0 (\bar{\mathcal{L}}_0 - \bar{\lambda}_0) a_s^\dagger \right\rangle - G \left\langle \frac{\psi_0^3 [1 + C^2(1 - \psi_0^2)]}{k[1 - B_k^2(1 - \psi_0^2)]} a_s^\dagger \right\rangle \right\} = \langle \psi_0^2 \rangle a_{s0}(-\theta) e^{-ik\theta}, \tag{29}$$

where  $B_k^2 \equiv -\Delta\bar{\omega}_p^2/(4k)$ . In a generic case, the transverse profile of signal  $a_s^\dagger(\bar{x})$  is a superposition of the FMC and CMC.

In this section, we fix  $a_s^\dagger(\bar{x}, \theta, k) \equiv A(\theta, k)\psi_0(\bar{x})$  for all instants of time [hence,  $(\bar{\mathcal{L}}_0 - \bar{\lambda}_0)a_s^\dagger = 0$  in Eq. (29)] and get finally

$$\frac{\partial A}{\partial \theta} + \bar{\gamma}_{\text{hom}}^2 \left( \frac{Q(k)}{2ik} \right) A = a_{s0}(-\theta) e^{-ik\theta}. \tag{30}$$

Here, the plasma response function [compare to Eq. (18)] reads

$$Q(k) = \int_{-1}^1 \frac{1 + C^2 y^2}{1 - B_k^2 y^2} (1 - y^2) dy. \tag{31}$$

In the SPWL regime (and, particularly, in its single-mode subregime which is considered here), relatively large wave number shifts,  $|k| \gg (\Delta\bar{\omega}_p/2)^2$  (that is,  $|B_k|^2 \gg 1$ ), contribute to the signal evolution. Hence, the main contribution to the integral (31) comes from the integrand values in the vicinity of  $y=0$  (or  $|y| \ll |B_k|^{-1}$ ). Approximating the integrand as  $(1 - B_k^2 y^2)^{-1}$  we find the approximate response function  $Q(k) \approx -2\pi\sqrt{k}/\Delta\bar{\omega}_p$  which allows to present Eq. (30) in the form

$$(\partial/\partial\theta + i\mathcal{W}k^{-1/2})A = a_{s0}(-\theta) e^{-ik\theta}, \tag{32}$$

where  $\mathcal{W} = \pi\bar{\gamma}_{\text{hom}}\sqrt{\bar{\gamma}_{\text{hom}}/(2\eta)}$ . Solution of Eq. (32) reads

$$A(\theta, k) = \int_0^\infty a_{s0}(\theta_1 - \theta) e^{-ik(\theta - \theta_1) - i\mathcal{W}\theta_1/\sqrt{k}} d\theta_1. \tag{33}$$

Inverting the Fourier transform (33) and returning to the lab-frame variables, we find the longitudinal evolution of the signal,  $A(\bar{z}, \bar{t}) = \int_0^\infty a_{s0}(\theta_1 + \bar{z})\mathcal{D}(\theta_1 - t, \theta_1)d\theta_1$ , where the Green function of RBS in the single-mode SPWL regime,  $\mathcal{D}(\theta_1 - t, \theta_1) = (2\pi)^{-1} \int_{-\infty}^{+\infty} \exp[ik(\theta_1 - t) - i\mathcal{W}\theta_1/\sqrt{k}]dk$ , is expressed in terms of the generalized hypergeometric function  ${}_1F_3$ :<sup>49</sup>

$$\mathcal{D}(\theta_1 - t, \theta_1) = \delta(t - \theta_1) + iH(t - \theta_1) \times (\mathcal{W}\theta_1)^2 {}_1F_3\left(\frac{1}{2}; 1, \frac{3}{2}, \frac{3}{2}; i\left(\frac{\mathcal{W}}{2}\right)^2 \theta_1^2(t - \theta_1)\right).$$

Then, the solution of initial-value problem reads

$$a_s^\dagger(\bar{x}, \bar{z}, \bar{t}) = \psi_0(\bar{x}) \left\{ a_{s0}(\bar{t} + \bar{z}) + i\mathcal{W}^2 \int_0^{\bar{t}} {}_1F_3\left(\frac{1}{2}; 1, \frac{3}{2}, \frac{3}{2}; i\left(\frac{\mathcal{W}}{2}\right)^2 \right) \times \theta_1^2(t - \theta_1) \right\} a_{s0}(\theta_1 + \bar{z}) \theta_1^2 d\theta_1. \tag{34}$$

Evolution of initially Gaussian signal  $a_{s0} = (u_0/10) \times \exp(-\bar{z}^2/100)$  is shown in Fig. 3 for the parameter set (I) of Fig. 1. Snapshots of the intensity profile  $|a_s(0, \bar{z}, \bar{t})|^2$  are presented for the three instants of time. The front of amplified pulse moves with a speed of light in the negative  $z$  direction, whereas the maximum moves with a group velocity  $v_g = -2c/3$ , as predicted in Sec. V A. The pulse maximum grows exponentially in time with an increment twice as given by Eq. (25). Therefore, the solution of initial-value problem confirms the predictions of dispersion analysis from Sec. IV.

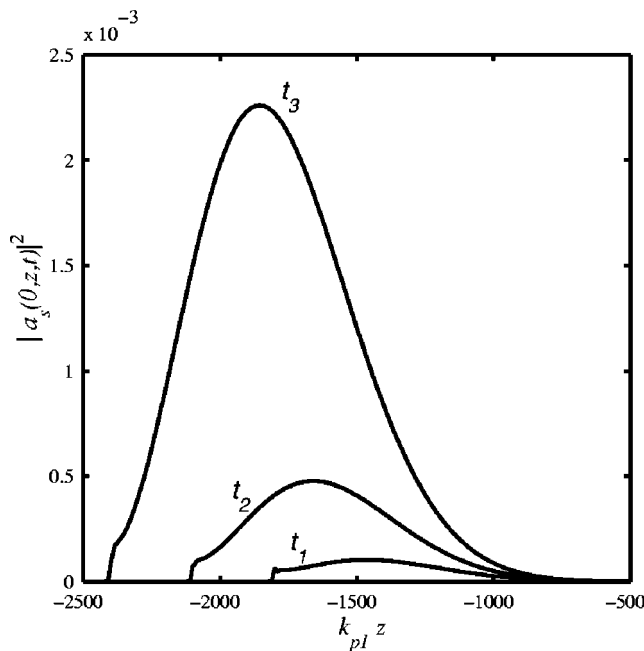


FIG. 3. Longitudinal on-axis profiles of intensity of the amplified signal for the parameter set (I) of Fig. 1,  $\bar{t}_1=1800$ ,  $\bar{t}_2=2100$ , and  $\bar{t}_3=2400$ . The seed signal is Gaussian,  $a_{s0}=(u_0/10)\exp(-z^2/100)$ .

## VI. CONCLUSION

We have investigated the RBS of laser radiation in the regime of SPWL in a plane plasma channel, which can support only one trapped EM mode (the single-mode channel<sup>42</sup>). For the SPWL regime, transverse variation of the plasma frequency exceeds the RBS bandwidth calculated for a homogeneous plasma with an on-axis electron density, and the scattering plasma wave is localized stronger than a driving beat wave of pump and scattered radiation. In this case, the transverse profile of scattered radiation is a superposition of the FMC and nonbound CMC. Depending on the plasma and laser parameters, the RBS with SPWL can proceed either in a single-mode or multimode regime. In the single-mode case, excitation of the CMC is suppressed almost completely, and only the FMC of scattered radiation is involved in the process. This allows for a physical analogy between the single-mode SPWL regime of RBS in a plasma channel and a three-wave RBS in a homogeneous plasma. In the multimode SPWL regime, the CMC play an essential role. The CMC contribution transversely shrinks the scattered radiation beam and increases the growth rate of instability. In both subregimes, the temporal growth rate is slower and amplification bandwidth is greater than in the case of homogeneous plasma, and the frequency spectrum experiences an overall redshift. The group velocity of scattered radiation,  $v_g \approx -2c/3$ , is increased versus its homogeneous-plasma value,  $v_{ghom}=-c/2$ . All these features are the consequences of the transverse shear of electron plasma density. The broadband nature of RBS in the SPWL regime and relatively high group velocity of scattered radiation are the features beneficial to the Raman amplification of short pulses in deep plasma channels.

## ACKNOWLEDGMENTS

This work was supported by the U.S. Department of Energy under Contracts No. DE-FG02-04ER54763 and No. DE-FG02-04ER41321.

## APPENDIX: PROPERTIES OF ASSOCIATED LEGENDRE FUNCTIONS WITH IMAGINARY ORDER

The associated Legendre functions  $P_1^{\pm iq}(y)$  (Ref. 50), where  $q$  is a positive real number, are the solutions (13) of Eq. (12) with  $s=1$  and  $\mu=\pm iq$ . The orthogonality condition for  $P_1^{\pm iq}(y)$  reads

$$\frac{1}{2\pi} \int_{-1}^1 P_1^{iq}(y) P_1^{-iq}(y) \frac{dy}{1-y^2} = \frac{\sinh(\pi q)}{\pi q} \delta(q' - q), \quad (\text{A1})$$

which is evaluated using the substitution  $y=\tanh(x/\sigma)$ , formulas (3.982) (3.987.1) and (3.981.6) (Ref. 47) and the Dirac delta-function property  $\delta(q' - q) = (2\pi)^{-1} \int_{-\infty}^{+\infty} e^{ix(q-q')} dx$ . The functions  $P_1^{\pm iq}(x)$  do not vanish at  $|x/\sigma| \rightarrow \infty$  and have the asymptotic

$$P_1^{iq}\left(\frac{x}{\sigma} \rightarrow +\infty\right) \sim \frac{e^{iqx/\sigma}}{\Gamma(1-iq)}, \quad (\text{A2a})$$

$$P_1^{iq}\left(\frac{x}{\sigma} \rightarrow -\infty\right) \sim \left(\frac{iq+1}{iq-1}\right) \frac{e^{-iq|x|/\sigma}}{\Gamma(1-iq)}. \quad (\text{A2b})$$

The cosine function can be constructed by summing up the even complex conjugate solutions  $\mathcal{P}_1^{iq}(x)=[P_1^{iq}(x)+P_1^{iq}(-x)]/2$  and  $\mathcal{P}_1^{-iq}(x)=[P_1^{-iq}(x)+P_1^{-iq}(-x)]/2$ :

$$\cos(qx/\sigma) = \left(\frac{\pi}{2}\right) \frac{(1+q^2)[P_1^{iq}(x)+P_1^{-iq}(x)]}{\text{Im} \Gamma(1+iq) + q \text{Re} \Gamma(1+iq)}.$$

<sup>1</sup>N. E. Andreev, Zh. Eksp. Teor. Fiz. **59**, 2105 (1970) [Sov. Phys. JETP **32**, 1141 (1971)].

<sup>2</sup>C. S. Liu, M. N. Rosenbluth, and R. B. White, Phys. Fluids **17**, 1211 (1974); J. F. Drake, P. K. Kaw, Y. C. Lee, G. Schmidt, C. S. Liu, and M. N. Rosenbluth, *ibid.* **17**, 778 (1974); W. M. Manheimer and E. Ott, *ibid.* **17**, 1413 (1974); D. W. Forslund, J. M. Kindel, and E. L. Lindman, *ibid.* **18**, 1002 (1975).

<sup>3</sup>W. L. Krueer, *The Physics of Laser Plasma Interactions* (Addison-Wesley, Reading, MA, 1988); Y. R. Shen, *Principles of Nonlinear Optics* (Wiley, New York, 1984).

<sup>4</sup>M. D. Perry and G. Mourou, Science **64**, 917 (1994), and references therein.

<sup>5</sup>C. B. Darrow, C. Coverdale, M. D. Perry, W. B. Mori, C. Clayton, K. Marsh, and C. Joshi, Phys. Rev. Lett. **69**, 442 (1992).

<sup>6</sup>C. Rousseaux, G. Malka, J. L. Miguel, F. Amiranoff, S. D. Baton, and Ph. Mounaix, Phys. Rev. Lett. **74**, 4655 (1995); V. Malka, E. De Wispelaere, J. R. Marques *et al.*, Phys. Plasmas **3**, 1682 (1996).

<sup>7</sup>A. Ting, K. Krushelnick, H. R. Burris, A. Fisher, C. Manka, and C. I. Moore, Opt. Lett. **21**, 1096 (1996).

<sup>8</sup>K. Krushelnick, C. I. Moore, A. Ting, and H. R. Burris, Phys. Rev. E **58**, 4030 (1998).

<sup>9</sup>X. F. Wang, R. Fedosejevs, and G. D. Tsakiris, Opt. Commun. **146**, 363 (1998).

<sup>10</sup>T. G. Jones, K. Krushelnick, A. Ting, D. Kaganovich, C. I. Moore, and A. Morozov, Rev. Sci. Instrum. **73**, 2259 (2002).

<sup>11</sup>V. K. Tripathi and C. S. Liu, Phys. Fluids B **3**, 468 (1991).

<sup>12</sup>C. J. McKinstrie and R. Bingham, Phys. Fluids B **4**, 2626 (1992).

<sup>13</sup>T. M. Antonsen, Jr. and P. Mora, Phys. Fluids B **5**, 1440 (1993).

<sup>14</sup>Ph. Mounaix, D. Pesme, W. Rozmus, and M. Casanova, Phys. Fluids B **5**, 3304 (1993); Ph. Mounaix and D. Pesme, Phys. Plasmas **1**, 2579 (1994).

<sup>15</sup>A. S. Sakharov and V. I. Kirsanov, Phys. Rev. E **49**, 3274 (1994).

- <sup>16</sup>N. E. Andreev, V. I. Kirsanov, and L. M. Gorbunov, *Phys. Plasmas* **2**, 2573 (1995).
- <sup>17</sup>G. Shvets, J. S. Wurtele, and B. A. Shadwick, *Phys. Plasmas* **7**, 1872 (1997).
- <sup>18</sup>G. Shvets, N. J. Fisch, A. Pukhov, and J. Meyer-ter-Vehn, *Phys. Rev. Lett.* **81**, 4879 (1998).
- <sup>19</sup>V. M. Malkin, G. Shvets, and N. J. Fisch, *Phys. Rev. Lett.* **82**, 4448 (1999).
- <sup>20</sup>Y. Ping, W. Cheng, S. Suckewer, D. Clark, and N. Fisch, *Phys. Rev. Lett.* **92**, 175007 (2004) and references therein; G. Shvets, S. Kalmykov, M. Dreher, and J. Meyer-ter-Vehn, *Bull. Am. Phys. Soc.* **48**, 77 (2003).
- <sup>21</sup>N. H. Burnett and G. D. Enright, *IEEE J. Quantum Electron.* **QE-26**, 1797 (1990).
- <sup>22</sup>X. F. Li, A. L'Huillier, M. Ferray, L. A. Lompré, and G. Mainfray, *Phys. Rev. A* **39**, 5751 (1989).
- <sup>23</sup>T. Tajima and J. M. Dawson, *Phys. Rev. Lett.* **67**, 243 (1979); E. Esarey, P. Sprangle, J. Krall, and A. Ting, *IEEE Trans. Plasma Sci.* **PS-24**, 252 (1996).
- <sup>24</sup>A. Modena, Z. Najmudin, A. E. Dangor *et al.*, *Nature (London)* **377**, 606 (1995); V. Malka, S. Fritzler, E. Lefebvre *et al.*, *Science* **298**, 1596 (2002); S. Fritzler, K. Ta Phuoc, V. Malka, A. Rousse, and E. Lefebvre, *Appl. Phys. Lett.* **83**, 3888 (2003); S. Fritzler, E. Lefebvre, V. Malka *et al.*, *Phys. Rev. Lett.* **92**, 165006 (2004); S. Mangles, B. Walton, M. Wei *et al.*, *Bull. Am. Phys. Soc.* **48**, 349 (2003).
- <sup>25</sup>C. G. Durfee, J. Lynch, and H. M. Milchberg, *Phys. Rev. E* **51**, 2368 (1995).
- <sup>26</sup>Y. Ehrlich, C. Cohen, A. Zigler, J. Krall, P. Sprangle, and E. Esarey, *Phys. Rev. Lett.* **77**, 4186 (1996).
- <sup>27</sup>P. Volfbeyn, E. Esarey, and W. Leemans, *Phys. Plasmas* **6**, 2269 (1999).
- <sup>28</sup>S. P. Nikitin, I. Alexeev, J. Fan, and H. M. Milchberg, *Phys. Rev. E* **59**, R3839 (1999).
- <sup>29</sup>E. W. Gaul, S. P. LeBlanc, A. R. Rundquist, R. Zgadzaj, H. Landhoff, and M. C. Downer, *Appl. Phys. Lett.* **77**, 4112 (2000).
- <sup>30</sup>T. C. Chiou, T. Katsouleas, C. Decker, W. B. Mori, J. S. Wurtele, G. Shvets, and J. J. Su, *Phys. Plasmas* **2**, 310 (1995).
- <sup>31</sup>G. Shvets, J. S. Wurtele, T. C. Chiou, and T. Katsouleas, *IEEE Trans. Plasma Sci.* **PS-24**, 351 (1996).
- <sup>32</sup>N. E. Andreev, L. M. Gorbunov, V. I. Kirsanov, K. Nakajima, and A. Ogata, *Phys. Plasmas* **4**, 1145 (1997).
- <sup>33</sup>G. Shvets and X. Li, *Phys. Plasmas* **6**, 591 (1999).
- <sup>34</sup>G. Shvets and J. S. Wurtele, *Phys. Rev. Lett.* **73**, 3540 (1994).
- <sup>35</sup>E. Valeo, *Phys. Fluids* **17**, 1391 (1974).
- <sup>36</sup>N. E. Andreev, L. M. Gorbunov, V. I. Kirsanov, A. A. Pogosova, and A. S. Sakharov, *Plasma Phys. Rep.* **22**, 379 (1996); N. E. Andreev, V. I. Kirsanov, L. M. Gorbunov, and A. S. Sakharov, *IEEE Trans. Plasma Sci.* **PS-24**, 363 (1996).
- <sup>37</sup>E. Esarey, C. B. Schroeder, B. A. Shadwick, J. S. Wurtele, and W. P. Leemans, *Phys. Rev. Lett.* **84**, 3081 (2000).
- <sup>38</sup>P. Sprangle, B. Hafizi, and J. R. Peñano, *Phys. Rev. E* **61**, 4381 (2000).
- <sup>39</sup>P. Sprangle, B. Hafizi, J. R. Peñano *et al.*, *Phys. Rev. E* **63**, 056405 (2001).
- <sup>40</sup>J. R. Peñano, B. Hafizi, P. Sprangle, R. F. Hubbard, and A. Ting, *Phys. Rev. E* **66**, 036402 (2002).
- <sup>41</sup>T. M. Antonsen, Jr. and P. Mora, *Phys. Rev. Lett.* **74**, 4440 (1995).
- <sup>42</sup>G. Shvets and X. Li, *Phys. Plasmas* **8**, 8 (2001).
- <sup>43</sup>C. J. McKinstrie, A. V. Kanaev, and E. J. Turano, *Phys. Rev. E* **56**, 1032 (1997); E. J. Turano and C. J. McKinstrie, *Phys. Plasmas* **7**, 5096 (2000).
- <sup>44</sup>S. C. Wilks, W. L. Krueer, E. A. Williams, P. Amendt, and D. C. Eder, *Phys. Plasmas* **2**, 274 (1995).
- <sup>45</sup>D. F. Gordon, B. Hafizi, P. Sprangle, R. F. Hubbard, J. R. Penano, and W. B. Mori, *Phys. Rev. E* **64**, 046404 (2001).
- <sup>46</sup>G.-Z. Sun, E. Ott, Y. C. Lee, and P. Guzdar, *Phys. Fluids* **30**, 526 (1987).
- <sup>47</sup>I. S. Gradshteyn and I. M. Ryzhik, *Table of Integrals, Series, and Products* (Academic, San Diego, 1994).
- <sup>48</sup>A. Bers, in *Handbook of Plasma Physics*, Basic Plasma Physics Vol. 1, edited by M. N. Rosenbluth and R. Z. Sagdeev (North-Holland, New York, 1983), p. 451.
- <sup>49</sup>E. W. Weisstein, *Generalized Hypergeometric Function*. From MathWorld-A Wolfram Web Resource, <http://mathworld.wolfram.com/GeneralizedHypergeometricFunction.html> (Wolfram Research, Inc., 100 Trade Center Drive, Champaign, IL 61820-7237, USA).
- <sup>50</sup><http://functions.wolfram.com/07.08.03.0012.01> (Wolfram Research, Inc., 100 Trade Center Drive, Champaign, IL 61820-7237, USA).